

**Combustion and Propulsion Research Laboratory
Mechanical and Industrial Engineering Department
The University of Texas at El Paso
El Paso, TX 79968**

**Final Technical Report on
Department of Energy Grant DE-FG26-06NT42749**

Entitled

Flame Synthesis of Carbon Nanotubes Using Low Calorific Value Gases

Authors

**Jorge Camacho, PhD
Mahesh Subramanya, PhD
Ahsan R. Choudhuri, PhD**

June 2007

Disclaimer

This report was prepared as an account of work sponsored by an agency of the United States Government. Neither the United States Government nor any agency thereof, nor any of their employees, makes any warranty, express or implied, or assumes any legal liability or responsibility for the accuracy, completeness, or usefulness of any information, apparatus, product, or process disclosed, or represents that its use would not infringe privately owned rights. Reference herein to any specific commercial product, process, or service by trade name, trademark, manufacturer, or otherwise does not necessarily constitute or imply its endorsement, recommendation, or favoring by the United States Government or any agency thereof. The views and opinions of authors expressed herein do not necessarily state or reflect those of the United States Government or any agency thereof.

Project Information

Project Title: Flame Synthesis of Carbon Nanotubes Using Low Calorific Value Gases

Grant No: DE-FG26-06NT42749

Agency: National Energy Technology Laboratory, Department of Energy

DOE Project Manager: John Stipanovich
U.S. Department of Energy
National Energy Technology Laboratory
Phone: (412) 386 6027
Email: John.Stipanovich@netl.doe.gov

Project Period: 03/17/06-03/17/07

Principal Investigator: Ahsan R. Choudhuri, PhD
Associate Professor (Research) and Director
Combustion and Propulsion Research Laboratory
Department of Mechanical and Industrial Engineering
The University of Texas at El Paso
500 West University, Mail Stop: 0521, El Paso, Texas 79968
Tel: 915 747 6905, Fax: 915 747 5019, E-mail: ahsan@utep.edu

Research Assistants: Jorge Camacho, PhD
Mahesh Subramanya, PhD

Preface

This is the final technical report on DOE Grant DE-FG26-06NT42749 entitled "Flame Synthesis of Carbon Nanotubes Using Low Calorific Value Gases". Technical work supported by this grant described in parts in doctoral dissertations of Jorge Camacho and Mahesh Subramanya. The results presented in the report are also included in a journal article titled "*Effects of Fuel Compositions on the Structure and Yield of Flame Synthesized Carbon Nanotube,*" *Fullerenes Nanotubes and Carbon Nanostructures*, Vol 15(2007), No. 2, pp. 99-112 . The paper is coauthored by Dr. Jorge Camacho and Dr. Ahsan Choudhuri. Another manuscript is currently in preparation for the same journal. The authors also gratefully acknowledge the contributions of Dr. Felicia Manciu in performing the Raman spectroscopy of the samples.

Abstract

Nanostructures formed in diffusion flames of pure fuels [CH_4 , C_3H_8 , and C_2H_2] at different fuel flow rates have been analyzed. Synthesis samples have been also collected from diffusion flames of various fuel blends [H_2 - CH_4 , H_2 - CO , H_2 - C_3H_8 , H_2 - C_2H_2] at different combustion conditions. SEM images of particulate samples collected from H_2 - CH_4 diffusion flames show formation of nanostructures. However, the formation of nanostructures only occurs at a narrow window of fuel compositions ($< 10\%$ H_2 concentration in the mixture) and flow conditions (Jet Exit Reynolds number $\text{Re}_j = 200$). At higher H_2 concentration and flow velocity, formation of nanostructures diminishes and H_2 - CH_4 flames produce amorphous carbon and soot particles.

Executive Summary

This proposed exploratory research project developed a flame synthesis technique of carbon nanotubes (CNTs) using low calorific value gases (LCVGs). A Cost effective and scalable CNT production methodology significantly benefits the affordable technology development for next generation sensors, gas storage mediums and high temperature materials required for the improvement of coal utilizations and production of premium fuels from coals. In addition the utilization of LCVGs for synthesizing CNTs enhances techniques for generating saleable by-products from waste streams and fuel gases in coal utilization processes through byproduct synergisms.

The proposed exploratory research has accomplished two primary objectives: (i) identification of the favorable flame conditions of low calorific value gases (LCVG) to produce carbon nanotubes, and (ii) demonstration of the feasibility of increasing the yield of the synthesis process using flow-field modifications.

Distinctive carbon nanostructures were produced depending on fuel types and fuel flow rates. The qualitative and quantitative analysis of many transmission electron microscope (TEM) and scanning electron microscope (SEM) images were performed.

Methane produced thin multi wall carbon nanotubes as well as nanorods and nanofibers within the fuel flow rate range of $7.18\text{E-}07$ m³/s to $9.57\text{E-}07$ m³/s. Propane yielded nanotubes only at the fuel flow rate of $4.20\text{E-}07$ m³/s. The nanotubes synthesized by acetylene flames were of different types that included helically coiled and twisted nanotubes.

SEM images of particulate samples collected from H₂-CH₄ diffusion flames show formation of nanostructures. The formation of nanostructures only occurs at a narrow window of fuel compositions (< 10% H₂ concentration in the mixture) and flow conditions (Jet Exit Reynolds number $Re_j = 200$). At higher H₂ concentration and flow velocity, formation of nanostructures diminishes and H₂-CH₄ flames produce amorphous carbon and soot particles.

Table of Contents

Project Information	i
Preface.....	ii
Abstract.....	iii
Executive Summary	iv
Table of Contents	v
I. Overview	1
II. Methodology	3
II.a. Synthesis Reactor.....	3
II.b. Qualification Tests	5
III. Results.....	6
III.a. Flame Characterization	6
III.b. Effects of fuel type and fuel flow rate.....	6
III.c. Effects of reaction time	17
III.d. Effects of Flow-Field.....	17
IV. Concluding Remarks.....	19
V. Bibliography.....	20

I. Overview

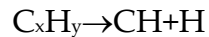
Carbon nanotubes (CNT) have distinct mechanical and electrical characteristics and are highly suitable for many novel technological applications such as high energy density batteries, gas storage medium for hydrogen and methane, high selectivity sensors, ingredients for high temperature composites etc [1-4].

Flame synthesis is an attractive method to produce carbon nanotubes in bulk quantities for commercial uses. It can be a very effective process since the fuel serves as both the heating and the reactant source and the synthesis process is highly scalable. Thus unlike methods such as laser ablation of composite metal-graphite targets, the flame synthesis of carbon nanotubes does not require large energy input and expensive infrastructures [5-6]. Although several recent investigations have reported the flame synthesis of carbon nanotubes [7-11], the nanotube yield was found to be too little to make the process commercially feasible. This is because the processes leading to the formation of carbon nanotubes during combustion of carbonaceous fuels are still not well understood.

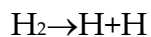
In a flame environment, the complex interactions of chemical kinetics and local flow quantities pose a difficult challenge to control the formation and the yield of nanotubes. For example, the fuel molecular constitution and the flame temperature govern soot and nanotubes formation in laminar diffusion flames [12]. A detailed discussion of fuel molecular structures and their possible effects on the nanostructure formation in flames through soot formation pathways are presented elsewhere [13]. Thus a systematic understanding of the effects of fuel types on the formation mechanism of flame structures will allow better optimizing the synthesis process. Motivated by this issue, the present work presents the effects of fuel type and flow rate on the formation of flame synthesized carbon nanostructures. Different types of carbon nanostructures were synthesized on galvanized iron catalyst using methane (CH_4), propane (C_3H_8) and acetylene (C_2H_2) diffusion flames.

The LCVG fuels are actually fuel blends and, in many aspects, the combustion of a fuel blend is different from that of its base fuels. In addition the LCVG fuels contain significant amount of hydrogen. The interactions of different chemical kinetics of each primary fuel of the fuel blend along with the flow dynamics significantly alter the combustion characteristics. For instance, hydrocarbon fuels have specific reaction routes to complete combustion and hydrogen chemistry

already embedded in the hydrocarbon reaction mechanism. However, the presence of additional hydrogen as a fuel in a LCV fuel changes the order of importance, or more specifically sensitivity of certain elementary reactions. The formation and destruction of H atom are important throughout the combustion process of hydrocarbon fuels. In typical hydrocarbon fuel combustion, the H atom forms through an initial global reaction and is given by



and then serves as a chain carrier. However, if hydrogen is present in the fuel along with other hydrocarbon fuels, another initial global reaction for hydrogen reaction becomes active



The addition of this reaction as an initial global reaction changes the priority of the reaction mechanism. For instance it influences the hydrocarbon reaction mechanism by accelerating the CH_3 consumption reaction ($CH_3 + H \leftrightarrow CH_2 + H_2$, $CH_3 + H \leftrightarrow CH_4$, $CH_3 + H_2 \leftrightarrow CH_4 + H$) without waiting to have sufficient H supplied from the initial hydrocarbon fuel breakup. Furthermore, the increase of CH_3 consumption gives an additional boost to fuel break up. Hence the effects of hydrogen addition become dominant because of the complex propagation of the reaction mechanism.

The above observation was evident in a series of previous investigations conducted by the principal investigator of the project [14-15]. It was also observed that a non-linear correlation exists between the volumetric concentration of hydrogen in the fuel mixture and the in flame production of OH, CH, H and O radicals and atoms [14-15]. This correlation can be effectively used to tailor the local chemistry towards the favorable flame condition of carbon nanotube formation. For example, based on this correlation, an optimum mixture of methane-hydrogen-carbon monoxide can be derived for a given catalyst to maximize the yield of flame synthesized nanotubes. The addition of hydrogen especially helps to achieve better control over the formation and destruction of OH and CH radicals which are two most important intermediates in combustion reaction mechanism.

II. Methodology

II.a. Synthesis Reactor

The synthesis reactor [Figure 1] was modified to mix and to meter the low Calorific value (LCV) gases into the reaction zone. The primary component of the reactor is a stainless steel tubular burner with a length/diameter ratio of 20 and an exit diameter of 1.8 mm which is connected inside a closed optically accessible combustion chamber. To introduce a modified flame flow-fields the reactors can also accommodate another circular burner with slotted exit. The slotted burner is capable of generating a known amount of turbulence in the vicinity of the nanotube formation zone [13]. The aluminum walled combustion chamber has three windows to provide optical access for non-intrusive flow diagnostic methods. Experiments are supported by air and fuel intake systems,

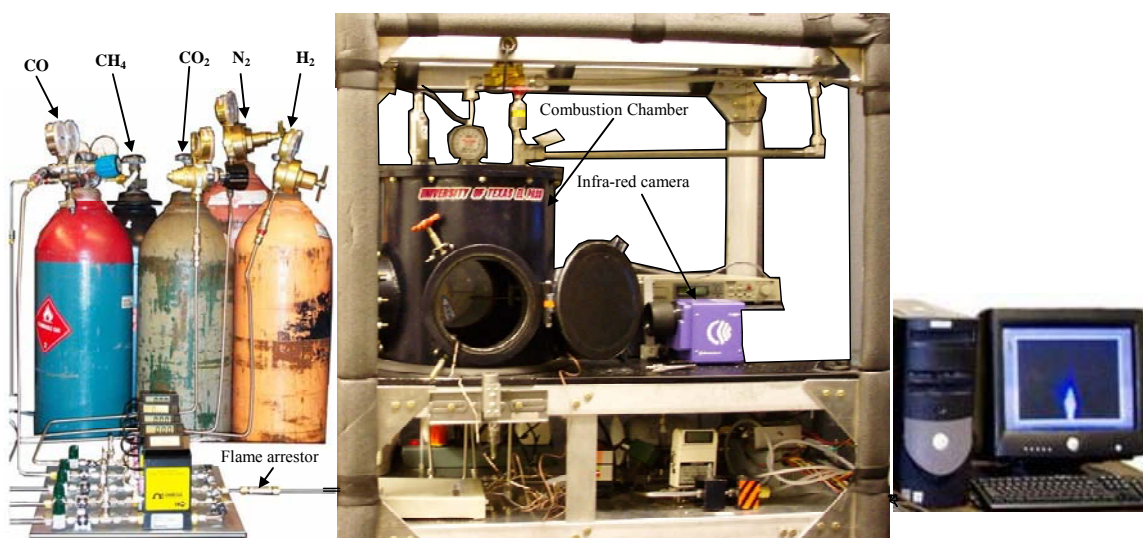


Figure 1: Nanotube Synthesis Reactor System

air exhaust systems, and safety systems and data acquisition instrumentation. The air intake and air exhaust systems were designed to maintain a constant pressure level inside the combustion chamber. During a typical run the flame inside the chamber burnt only 5-8% of the chamber air. Two remotely operated spark igniters initiated the combustion process. The details of the reactor can be found elsewhere [13].

To mix and meter different gases for simulating LCV fuels a mixing manifold fitted with a bank of flowcontrollers has been installed [Figure 2]. The flow

controllers consist of digital flow meters [thermal conductive] and precision needle valves. Different gases are fed into the inlet of the controllers using high pressure gas cylinders and two-stage regulators.

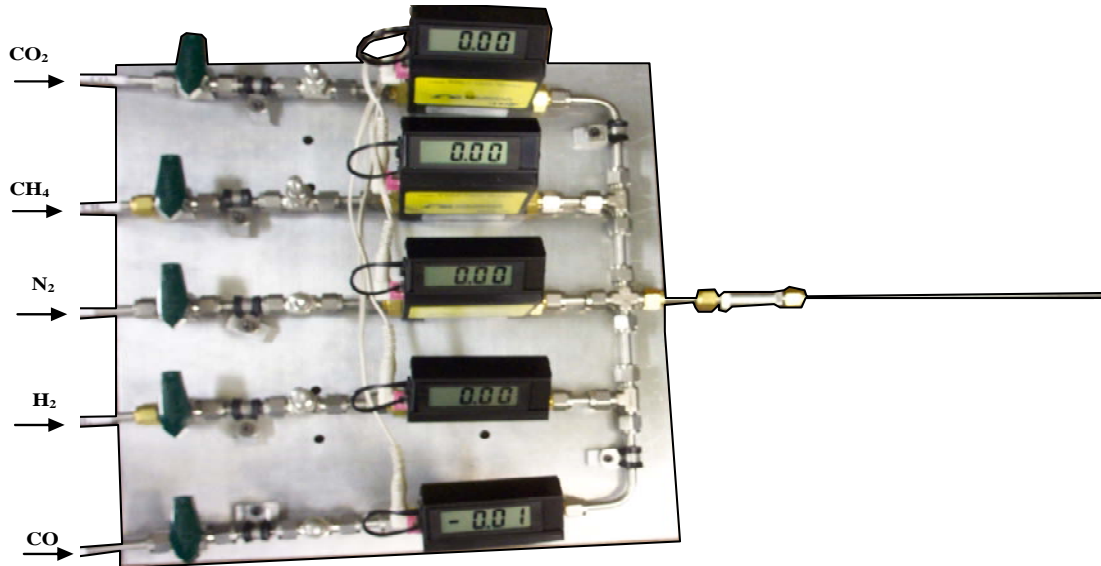


Figure 2a: Fuel Metering and Mixing Manifold

Fig. 2b shows a schematic representation of the sample collector system. The grid-clamp is mounted on a double-acting pneumatic system designed to minimize the disturbances of the collector system on flame front. Pneumatic cylinder 1 is designed to move a distance of one-inch in the short sampling time and pneumatic cylinder 2 is designed to move over nine-inches at a very slow pace.

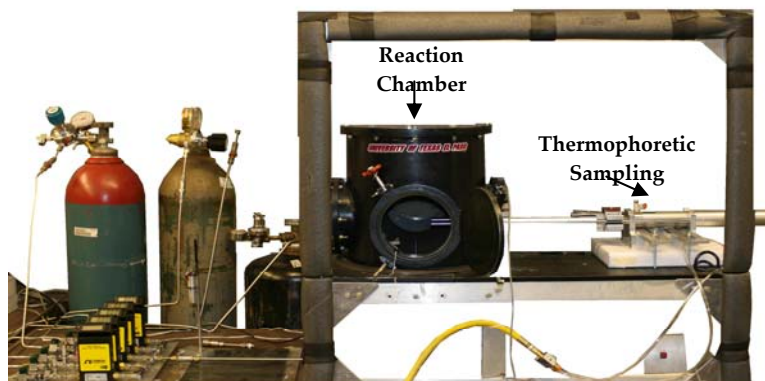


Fig. 2b Experimental Setup with Thermophoretic Sampling Technique

II.b. Qualification Tests

Diffusion flames for jet ext Reynolds number of ~200, ~400, and ~600 and various compositions of LCV fuels were established to understand the flame characteristics. **Table 1**¹ lists the compositions used for the present investigation. High quality digital and thermal images were taken to understand the structure the flames. The particular Reynolds number range [200-600] was selected based on the previous experience with pure fuels such methane, propane and acetylene [13]. It was observed that a narrow flame zone [predominantly blue inception zone] prior to the soot growth section of the flame yields most of the flame synthesis nanotubes. The purpose of the qualification tests was to establish and to characterize (thermal structure) those zones in LCV fuel flames.

Gasification	Type of coal	CO (%)	H ₂ (%)	CH ₄ (%)	N ₂ (%)	CO ₂ (%)	Calorific Value (MJ/m ³)
Coal	Brown coal	16	25	5	40	14	6.28
	Bituminous	17.2	24.8	4.1	42.7	11	6.13
	Lignite	22	12	1	55	10	4.13
	Coke	29	15	3	50	3	6.08

¹ The information in Table 1 is compiled from the article Chomiak, J., Longwell, J. P., and Sarofim (1989) "Combustion of Low Calorific Value Gases: Problems and Prospects," *Prog. Energy Combust. Sci.*, Vol. 15, pp. 109-129.

III. Results

III.a. Flame Characterization

Flame Characteristics: **Figures 3-6** shows the flame images of different LCV fuels [Coal Gas: Brown, Bituminous, Lignite and Coke] at different Reynolds numbers. It appears that for same Reynolds number Brown and Bituminous coal gas flames have higher soot inception zones in compared to Lignite and Coke coal gas. The thermal structures of these gases are also more favorable to the nanotube growth.

III.b. Effects of fuel type and fuel flow rate

Methane (CH_4) produced thin multi-wall carbon nanotubes as well as nanorods and nanofibers. The production of nanotubes was limited to fuel flow rates of $7.18\text{E-}07 \text{ m}^3/\text{s}$ to $9.57\text{E-}07 \text{ m}^3/\text{s}$. Nanofibers [**Figure 7**] were observed at low fuel flow rate ranging from $5.98\text{E-}07$ to $7.18\text{E-}07 \text{ m}^3/\text{s}$. Long and short multi-wall nanotubes [**Figure 8**] in the range of 9 to 15 nm in diameter were synthesized at a fuel flow rate of $8.37\text{E-}07 \text{ m}^3/\text{s}$. The quantity of nanotubes yielded by methane flames was limited in compared to those produced by acetylene flames. At higher fuel flow rates nests of carbon strings or fibers forming large webs were observed [**Figure 9**]. In addition, graphite nanocrystals and some particulate nucleation were also observed in methane flames.

Propane (C_3H_8) flames produced nanotubes for a limited range of fuel flow rates (around $4.20\text{E-}07 \text{ m}^3/\text{s}$). However, nanofibers or nanotubes at their early stage of inception processes were identified at a fuel flow rate close to $3.00\text{E-}07 \text{ m}^3/\text{s}$ [**Figure 10**]. In general, carbon nanotubes produced by propane flames have diameters in between 30 to 80 nm. Nanotubes formed in propane flames are straight and bundled parallel to each other. In addition, fullerenes and twisted nanotubes were observed in propane flames [**Figure 11**]. However, the twisted nanotubes did not show any evidence of fractures or defects. At higher fuel flow rates, nanofibers and porous carbon structures composed of interconnected nanofibers were also observed [**Figure 12**].





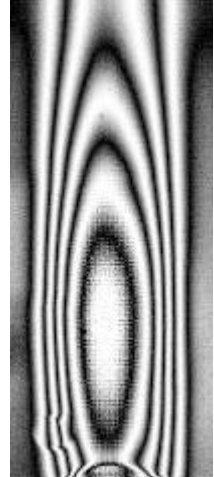
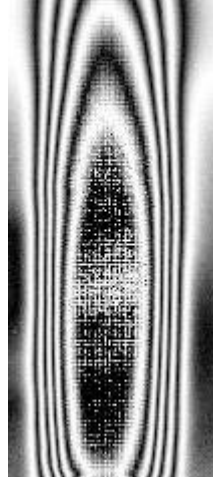
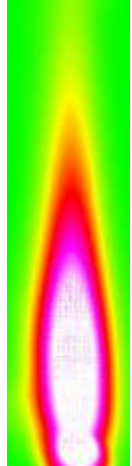
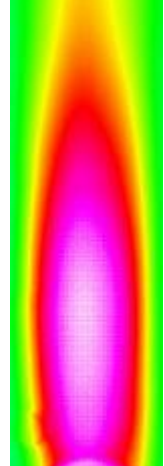

Composition	Flow rate (L/min) Re= 204	Flow rate (L/min) Re= 401	Flow rate (L/min) Re= 604
N2 (40%)	0.21	0.41	0.62
CO (16%)	0.08	0.16	0.25
CO2 (14%)	0.074	0.147	0.214
CH4 (5%)	0.028	0.050	0.079
H2 (25%)	0.131	0.252	0.384
Total	0.524	1.020	1.547
Color image			
Thermal Image (Slice 11 bit)			
Thermal Image (Spectrum 1)			

Figure 3: Flame images of brown coal gas





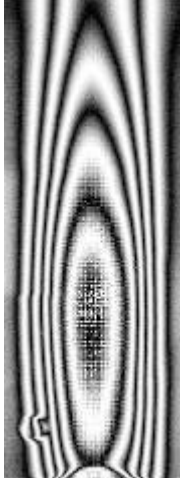
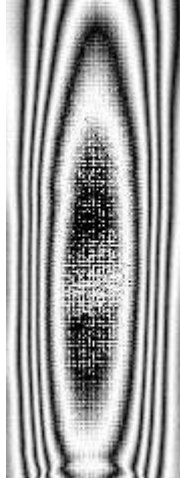
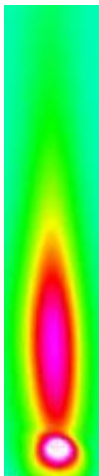
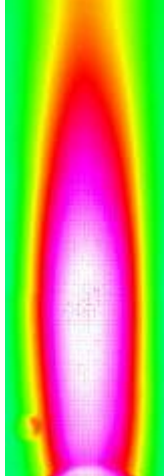
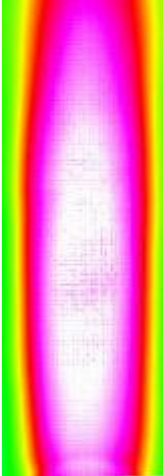
Composition	Flow rate (L/min) Re= 205	Flow rate (L/min) Re= 404	Flow rate (L/min) Re = 602
N2 (42.7%)	0.23	0.45	0.67
CO (17.2%)	0.09	0.18	0.27
CO2 (11%)	0.059	0.118	0.177
CH4 (4.1%)	0.029	0.050	0.072
H2 (24.8%)	0.131	0.263	0.394
Total	0.539	1.061	1.583
Color Image			
Thermal Image (Slice 11 bit)			
Thermal Image (Spectrum 1)			

Figure 4: Flame images of bituminous coal gas







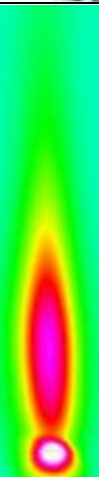


Composition	Flow rate (L/min) Re= 217	Flow rate (L/min) Re= 415	Flow rate (L/min) Re= 620
N2 (55%)	0.28	0.54	0.8
CO (22%)	0.11	0.21	0.32
CO2 (10%)	0.052	0.096	0.148
CH4 (1%)	0.0072	0.014	0.014
H2 (12%)	0.061	0.121	0.172
Total	0.509	0.982	1.454
Color image			
Thermal Image (Slice 11 bit)			
Thermal Image (Spectrum 1)			

Figure 5: Flame images of lignite coal gas





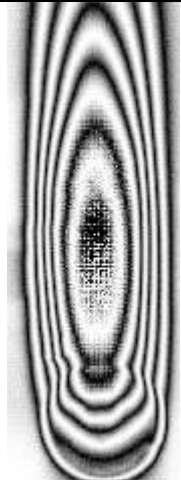
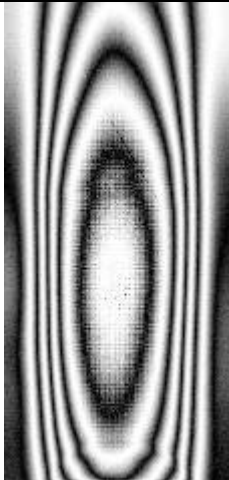
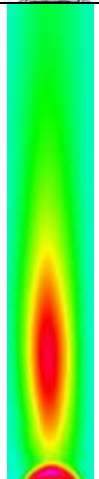
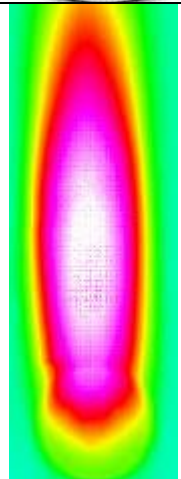
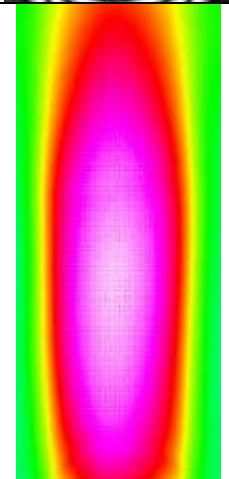
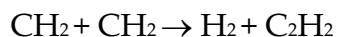
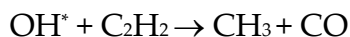
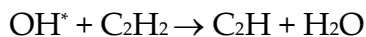
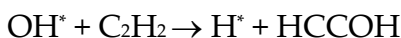
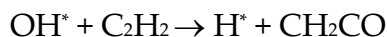
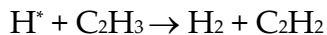
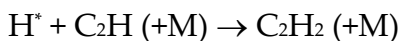
Composition	Flow rate (L/min) Re= 208	Flow rate (L/min) Re= 400 N_R	Flow rate (L/min) Re= 602
N2 (50%)	0.27	0.52	0.78
CO (29%)	0.16	0.3	0.45
CO2 (3%)	0.015	0.030	0.044
CH4 (3%)	0.014	0.029	0.050
H2 (15%)	0.081	0.162	0.232
Total	0.540	1.040	1.557
Color image			
Thermal Image (Slice 11 bit)			
Thermal Image (Spectrum 1)			

Figure 6: Flame images of coke coal gas

Acetylene (C₂H₂) produced different types of nanotubes including helically coiled carbon nanotubes in large quantities at different fuel flow rates [Figure 13]. Nanotubes were synthesized in acetylene flames for a wide range of fuel flow rates (4.83E-07 m³/s to 7.73E-07 m³/s). At higher flow rates ($\geq 8.70\text{E-}07$ m³/s) acetylene flames produced nanofibers and carbon structures that are porous or layered [Figure 14]. The higher yield of carbon nanotubes is inherently related to the soot formation mechanisms in acetylene flames [16]. An important class of soot precursor in flame environment is polycyclic aromatic hydrocarbons (PAH) and acetylene (C₂H₂), which is the most important precursor of PAHs. In hydrocarbon flames (other than acetylene), C₂H₂ formation process is related to the OH*, CH* and H* chemistry and is subjected to the rate coefficients of elementary reactions such as:



In contrast, acetylene fuel directly supplies C₂H₂ in the PAH growth zone. A typical PAH growth mechanism starts with the decomposition of C₃H₄ or reaction of CH* or CH₂ with C₂H₂ to C₃H₃, which can form the first ring (benzene C₆H₆) after recombination to an aliphatic C₆H₆ and rearrangement. A regular PAH formation pathway (condensation processes) such as this involves a large number of formation step and depends on the local stoichiometry of the flame. Since the formation of C₂H₂ in acetylene flames does not depend on any primary pyrolysis processes, it alters the PAH formation mechanisms greatly which in turns affects the growth chemistry of the nanotubes. It appears that a large supply of PAH in nanotube growth zone leads to the higher yield carbon nanotubes.

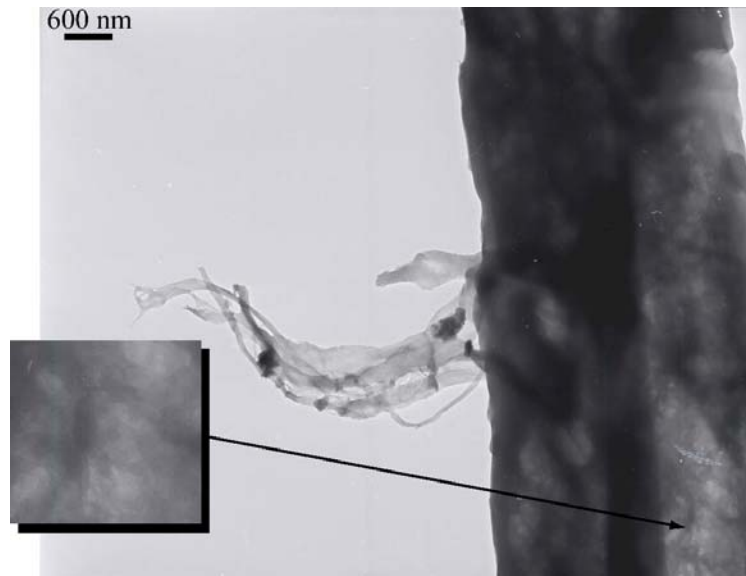


Figure 7. TEM image of carbon nanofibers and layers formed by methane at a flow rate of $5.98\text{E-}07\text{ m}^3/\text{s}$.

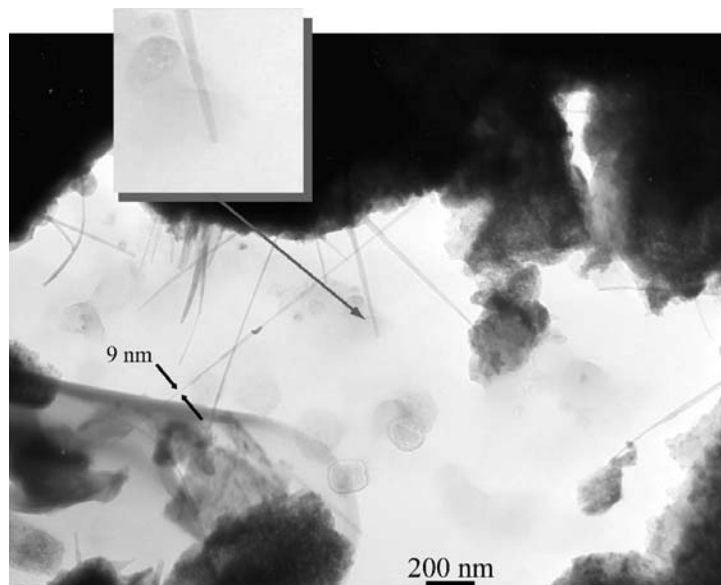


Figure 8. TEM images of carbon nanotubes formed by methane at a flow rate

of $8.37\text{E-}07 \text{ m}^3/\text{s}$.

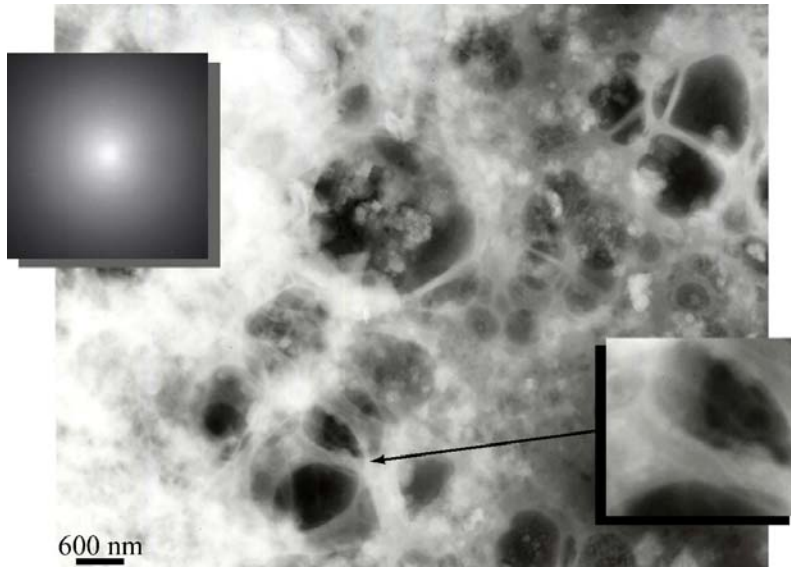


Figure 9. TEM images of likely graphite nanocrystals and a web of nanofibers (methane at a flow rate of $1.08\text{E-}6 \text{ m}^3/\text{s}$).

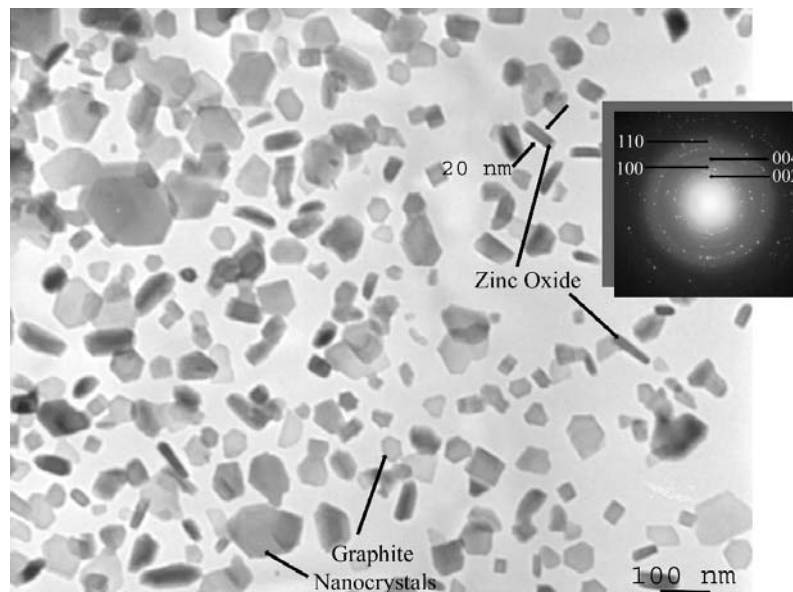


Figure 10. TEM image and diffraction pattern of graphite nanocrystals and possible nucleates of carbon nanotubes (propane at a flow rate of $3.60\text{E-}7 \text{ m}^3/\text{s}$).

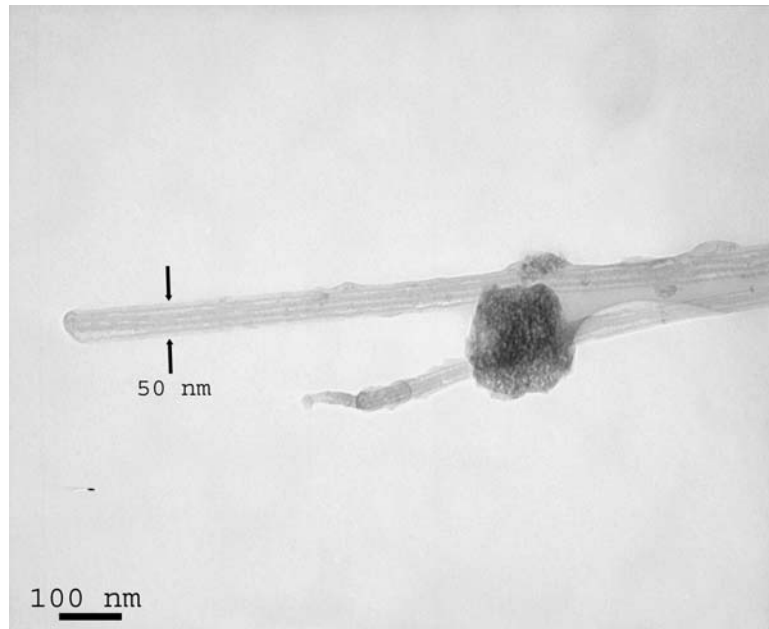


Figure 11. TEM images of carbon nanotubes and fullerenes (propane at a flow rate of $4.20\text{E-}7 \text{ m}^3/\text{s}$).



Figure 12. TEM images of porous carbon nanostructures containing nanofibers (propane at a flow rate of $5.40\text{E-}7 \text{ m}^3/\text{s}$).

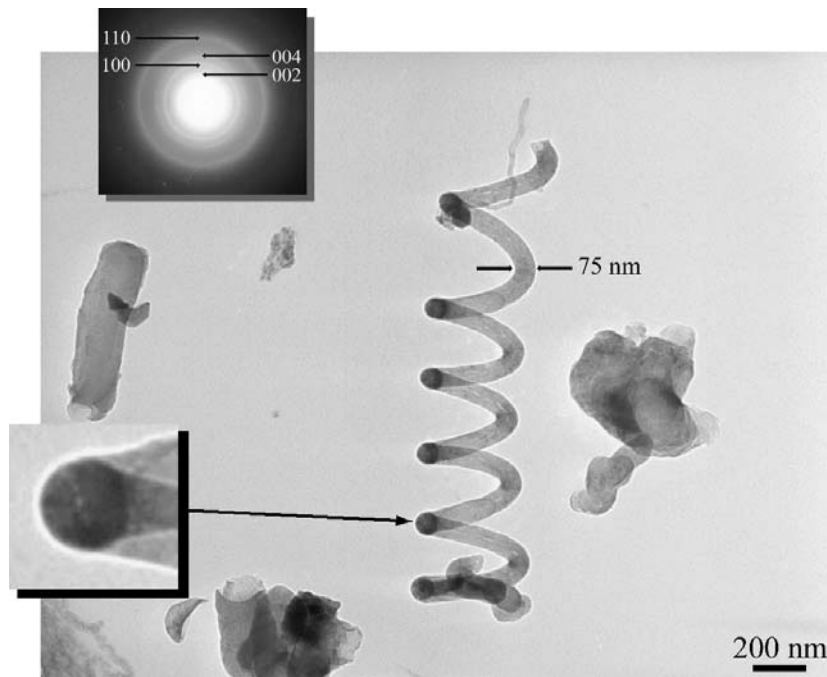


Figure 13. TEM image and diffraction pattern of a helically coiled carbon nanotube (acetylene at a flow rate of $4.83\text{E-}7 \text{ m}^3/\text{s}$).

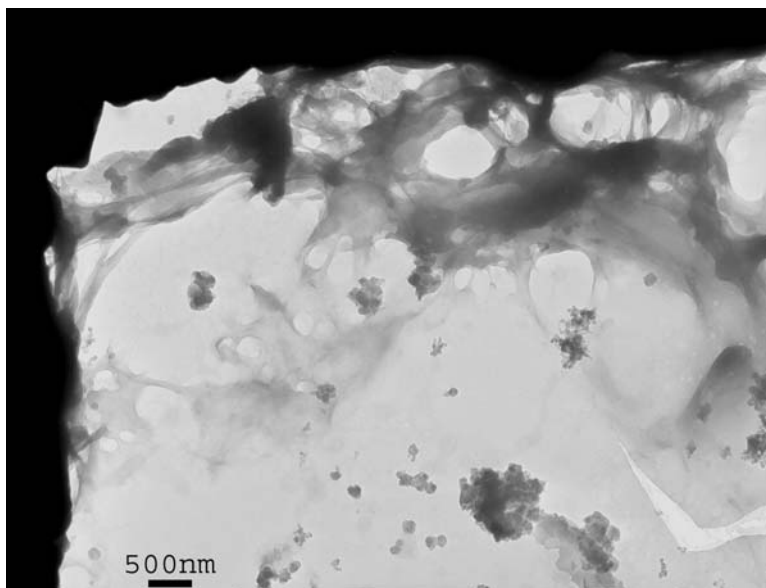


Figure 14. TEM image of possible porous carbon structures with soot (acetylene at a flow rate of $8.70\text{E-}7 \text{ m}^3/\text{s}$).

Figure 15 shows the SEM image of a particulate sample collected from a 5% H_2 -95% CH_4 fuel flame with a jet exit Reynolds number of 200. Using a thermophoretic sampling technique, particulates were sampled at a location 5 mm downstream of the burner exit.

The SEM image shows a substantial amount of straight nanotubes with an average diameter of 600 nm. The tubes are highly aligned and form a dense package of nanotubes. This type of synthesis is especially useful for creating sensor surfaces. Compared to 100% CH_4 fuel, nanotubes synthesized using 5% H_2 -95% CH_4 fuel blends are generally more straight and larger in length and diameter. Additionally, the yield of nanotubes is higher in H_2 - CH_4 flames.

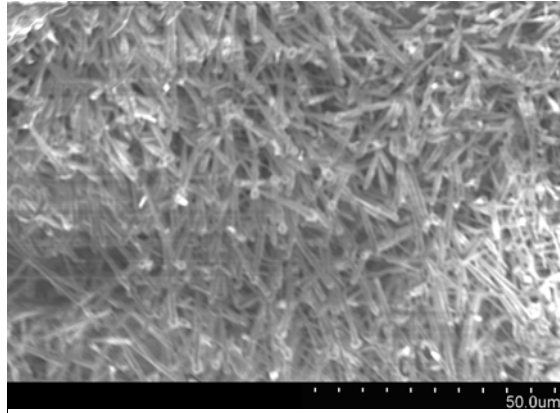


Figure 15: SEM image of long carbon nanotubes formed in a 5%-95% H_2 - CH_4 flame

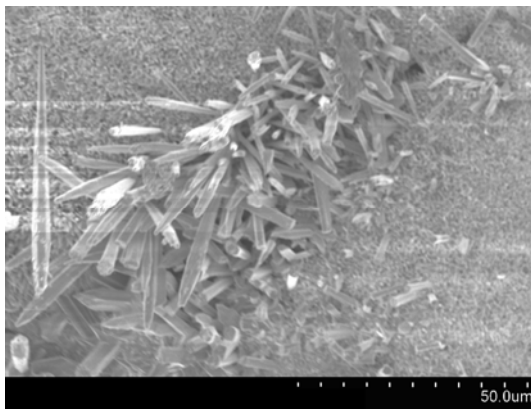


Figure 16: Growth of carbon nanotubes from an amorphous carbon bed

Figure 16 shows the growth of straight nanotubes from an amorphous carbon bed. The sample was collected from the same flame mentioned earlier. It is interesting to note that end caps of some of the nanotubes were snapped during the formation process. If the process can be reliably repeated this type of formation will enhance the selectivity of nanotube formed sensor surfaces.

The yield of nanotubes diminishes rapidly with the increase H_2 concentration in fuel mixtures. **Figure 17** shows the SEM image of a particulate sample collected from a 10% H_2 -90% CH_4 mixture. The sample is primarily composed of amorphous carbon flakes with a trace of nanotubes. With the further increase in H_2 concentration, dense clouds of granular carbon structures entirely replace amorphous carbon flakes

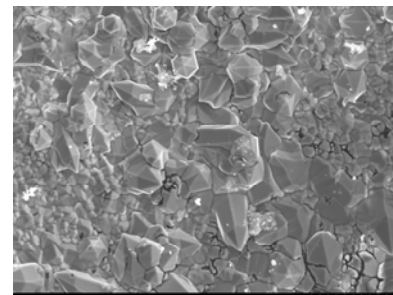


Figure17: SEM image of particulates formed in a 10%-90% H_2 - CH_4 flame

[Figure 18]. Currently Raman spectra of samples are being analyzed to further characterize the nanostructures.

III.c. Effects of reaction time

The time that the catalyst stays on the flame affects the growth of the carbon nanotubes. It was found that nanotubes grew in diameter and in length with the increase in reaction time. The carbon concentric layers were continuously added to the nanotube thus creating large tubes of about 400 to 500 nm in diameter. With the oxidation of galvanized steel the yield of nanotubes increased significantly. In addition, carbon fibers fully covered by other smaller fibers or carbon nanotubes are produced at large reaction times. **Figures 19-21** show the effects of reaction time on the formation of nanotubes in acetylene flames.

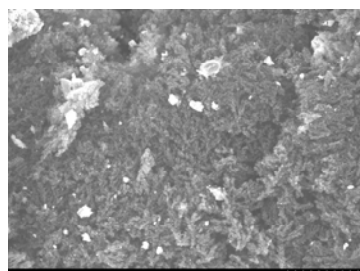


Figure 18: SEM image of particulates formed in a 15%-85% H₂-CH₄ flame

III.d. Effects of Flow-Field

The nozzle was modified to create a level of turbulence ($\pm 12\%$ of the mean flow) in the nanotube formation zone. The improved mixing due to local turbulence resulted reduced soot formation and yield more carbon nanotubes. At a fuel flow rate of $5.80\text{E-}07 \text{ m}^3/\text{s}$ and 4 sets of reaction time of 15 minutes tests, nanotube material produced by acetylene flame at laminar and turbulent conditions were about 8 mg and 20 mg respectively. The introduction of additional turbulence in formation zone increased the production of both straight and coiled carbon nanotubes. In addition, turbulent flames produced nanotubes in all fuel flow rates in contrast to laminar flames, which yielded nanotubes only up to the $7.73\text{E-}07 \text{ m}^3/\text{s}$ fuel flow rate. The turbulent effect created longer carbon nanotubes in length and changed the growth of the nanotube from straight to coil or vice versa (**see also reference [13]**). Furthermore, most of the nanotubes produced in turbulent flames did not have metal particles, which indicates that the introduction of turbulence in growth zone may prevent encapsulation of metal particles from the catalyst.

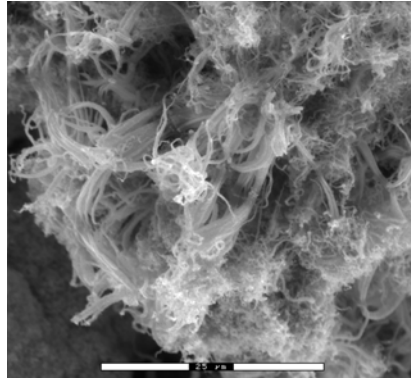


Figure 19. Tubes and fibers produced after 30 seconds of reaction time of the galvanized steel with acetylene (flow rate of $6.77\text{E-}07\text{ m}^3/\text{s}$).

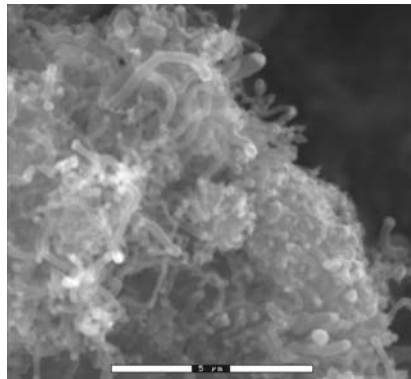


Figure 20. Carbon tubes produced after 5 minutes of reaction time of the galvanized steel with acetylene (flow rate of $6.77\text{E-}07\text{ m}^3/\text{s}$).

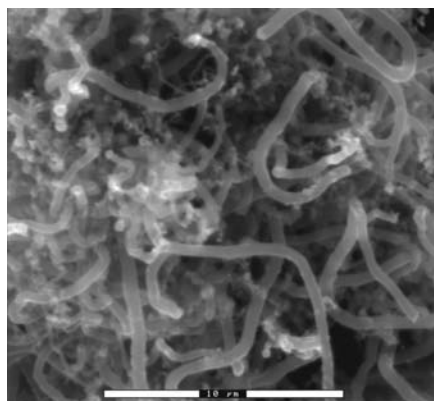


Figure 21. Tubes and fibers produced after 15 minutes of reaction time of the galvanized steel with acetylene (flow rate of $6.77\text{E-}07\text{ m}^3/\text{s}$).

IV. Concluding Remarks

Different types of carbon nanostructures were synthesized on galvanized iron catalyst using diffusion flames of two different types of fuel family i.e. pure [methane, propane, and acetylene and blends [hydrogen and methane]. The study concludes that the ability of a fuel to produce well resolved carbon nanostructures in flame environment is somewhat related to its molecular structure through its sooting propensity and flame temperature. For instance, acetylene has a maximum soot yield of 23% and it produces high yield of nanotubes for a wide range of flow rate. On the other hand propane has a maximum soot yield 16% and it produces carbon nanotubes only for a limited range of fuel flow rate.

Nanotubes synthesized using 5% hydrogen-95% methane fuel blends are generally more straight and larger in length and diameter in compared to 100% methane fuel. Additionally, the yield of nanotubes is higher in hydrogen-methane flames. However, the yield of nanotubes diminishes rapidly with the increase hydrogen concentration in fuel mixtures. The formation of nanostructures occurs at a narrow window of fuel compositions (< 10% hydrogen concentration in the mixture) and flow conditions (Jet Exit Reynolds number $Re = 200$).

The flow-field has a pronounced effect on the yield of the carbon nanotubes formation in flames. Regardless of the type, an introduction of turbulence in the nanotube formation zone of a flame enhances the yield. It appears that the perturbations in freestream flame conditions affect the temperature concentration and velocity gradient that can lead to a change in nanotube formation. If the region of a large fuel concentration could be shifted to high temperatures than the nanotubes inception chemistry can be accelerated.

V. Bibliography

- [1] Saito Y, Hamaguchi K, Hata K, Uchida K, Tasaka Y, Ikazaki F, Yumura M, Kasuya A, Nishina Y. *Conical Beams From Open Nanotubes*, 1997, *Nature*, vol. 389, pp. 554–555.
- [2] Dai HJ, Hafner JH, Rinzler AG, Colbert DT, Smalley RE. *Nanotubes as Nanoprobes In Scanning Probe Microscopy*, 1996, *Nature*, vol. 384, pp. 147–140
- [3] Tans S J, Verschueren ARM, Dekker C. *Room-Temperature Transistor Based on a Single Carbon Nanotube*, 1998, *Nature*, vol. 393, pp. 49–52.
- [4] Qian D, Dickey EC, Andrews R, Rantell T. *Load Transfer And Deformation Mechanisms In Carbon Nanotube–Poly- Styrene Composites*, 2000, *Appl Phys Lett*, vol. 76, pp. 2868–2870.
- [5] Vander Wal., Randall L., *Fe-Catalyzed Single-Walled Carbon Nanotube Synthesis within a Flame Environment*, 2002, *Combustion and Flame*, 2002, vol. 130, pp. 37–47.
- [6] Height, Murray J., Howard, Jack B., Tester, Jefferson W. and Vander Sande, John B., *Flame synthesis of Single-walled Carbon Nanotubes*, 2004 *Carbon*, vol. 42, pp. 2295-2307.
- [7] Yuan, Liming, Saito, Kozo, Hu, Wenchong and Chen, Zhi, *Ethylene Flame Synthesis of Well-Aligned Multi-Walled Carbon Nanotubes*, 2001, *Chemical Physics Letters*, vol. 346, pp. 23-28.
- [8] Yuan, Liming, Li, Tianxiang and Saito, Kozo, *Growth Mechanism of Carbon Nanotubes In Methane Diffusion Flames*, 2003, *Carbon*, vol. 41, pp. 1889-1896.
- [9] Vander Wal., Randall L., *Flame synthesis of Ni-catalyzed nanofibers*, 2003, *Carbon*, vol. 40, pp. 2101-2107. .
- [10] Vander Wal., Randall L., *Flame Synthesis of Substrate-Supported Metal-Catalyzed Carbon Nanotubes*, 2000, *Chemical Physics Letters*, vol. 324, pp. 217-223.
- [11] Vander Wal., Randall L., Ticich Thomas M. and Curtis Valerie E., *Diffusion Flame Synthesis of Single-Walled Carbon Nanotubes*, 2000, *Chemical Physics Letters*, vol. 323, pp. 217-223.
- [12] Gulder, Omer L., *Influence of Hydrocarbon Fuel Structural Constitution and Flame Temperature on Soot Formation in Laminar Diffusion Flames*, 1989, *Combustion and Flame*, vol. 78, pp. 179-194.
- [13] Camacho, J., *Flame Synthesis of Carbon Nanotubes*, PhD Dissertation, University of Texas at El Paso, El Paso, Texas (2005), Advisor Dr. Ahsan Choudhuri.

- [14] Choudhuri A. R. and Gollahalli, S.R. *Intermediate Radical Concentrations in Hydrogen-Natural Gas Blended Fuel Jet Flames*, 2004, International Journal of Hydrogen Energy, vol. 29, pp. 1293-1302
- [15] Choudhuri A. R. and Gollahalli, S.R. *Laser Induced Fluorescence Measurements of Radical Concentrations in Hydrogen-Hydrocarbon Blended Gas Fuel Flames*, 2000, International Journal of Hydrogen Energy, vol. 25, pp. 1119-1127.
- [16] Choudhuri, A. R., Camacho, J. and Chessa, J., *Flame Synthesis of Coiled Carbon Nanotubes*, 2006 Fullerenes Nanotubes and Carbon Nanostructures, vol 14., Number 1, pp. 93-100.